

Aqua-Quad - Solar Powered, Long Endurance, Hybrid Mobile Vehicle for Persistent Surface and Underwater Reconnaissance, Part I - Platform Design

Kevin Jones, Vladimir Dobrokhodov, Chase Dillard

Mechanical and Aerospace Engineering dept

Naval Postgraduate School

Monterey, California 93943

Email: jones@nps.edu, vldobr@nps.edu, chasedillard@gmail.com

Abstract—The development of a novel hybrid autonomous vehicle, Aqua-Quad, is presented, which combines a multi-rotor vertical take off and landing aircraft with environmentally hardened electronics, exchangeable sensor suite and a solar recharge system in order to provide long endurance sensing in aquatic environments in support of a variety of missions. The vehicle is envisioned to perform sensing below the thermocline while silently riding on ocean currents, and flying in the air when required for rapid relocation or local communication (12-20 miles) with similar cooperative nodes. The vehicle instrumentation combines (i) INS/GPS and aircraft control, data processing, and command and control (C2) capabilities of a VTOL aircraft, (ii) sensing and signal processing capabilities of an underwater robot with a vector sensor suspended below the thermocline, and (iii) solar energy harvesting for energy-independent operation. The Aqua-Quad is most effective when multiple cooperative vehicles are deployed in an operational area with heterogeneous sensors. It is envisioned that the extended endurance and quiet operation of the multi-modal sensing vehicles, capable of on-demand communication, higher mobility, and cooperative reaction to potential threats could provide higher operational efficiency of the system in undersurface surveillance and reconnaissance operations than currently employed systems (e.g., Sonobuoy, Wave Glider, etc.).

I. INTRODUCTION

There are a multitude of tasks, in all branches of the armed forces as well as the scientific community and private sectors that require persistent, wide-area sensing in virtually all environments, air, sea and land. On the ocean surface, buoys and disposable floaters are frequently used, but are subject to ocean currents, providing mobility, but not necessarily mobility in the desired direction. They typically provide limited sensing at or near the surface, and are usually limited to low-bandwidth satellite communications or data storage until they are retrieved. Underwater there are a few solutions. For example, sea gliders [1] provide long endurance and at least some mobility beyond ocean currents. However they are limited to undersea and surface sensing, and are typically out of communications most of the time, again limited to low-bandwidth communications when they are on the surface.

Wide area, long endurance coverage in the air is also challenging. One ongoing study, Tactical Long Endurance Unmanned Aerial System (TALUAS - pronounced *talus*) [2], proposes to utilize a flock of networked aircraft that use a combination of natural, convective lift in the environment

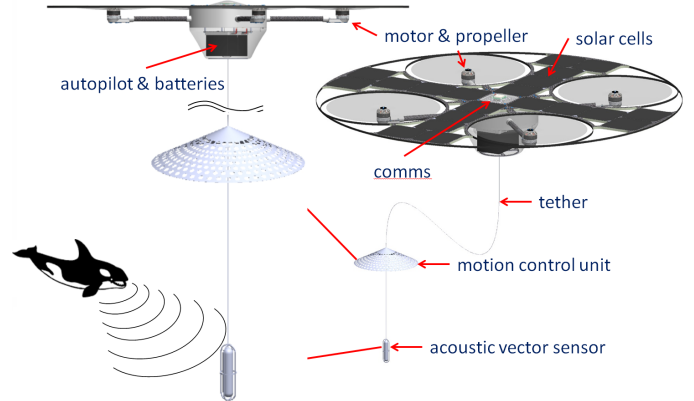


Fig. 1: AquaQuad conceptual design.

and photovoltaic (PV) cells coupled to high-energy density rechargeable batteries to provide 24/7 aerial coverage. While this concept is promising for aerial missions, ISR, communications-relay, etc, it is not of much use for sensing at the ocean surface, underwater, or ground sensing where severe proximity limitations exist, such as looking for mines buried in the beach.

None of these schemes are able to cover all environments, air/sea/ground, and each includes constraints for communications, mobility and/or survivability in harsh weather. The proposed concept, Aqua-Quad [3], [4] (see Fig.1), is a true hybrid platform, capable of use in all these environments, with both air and surface mobility, 24/7 sensing and high bandwidth communications. In this paper, a summary of the development of the prototype platform is given, with initial flight data and performance projections. The variety of potential mission sets where such a vehicle, or *flock* of vehicles, would be useful is extensive, and is presented in more detail in a companion paper at this conference [5].

A flock of vehicles might be outfitted with deployable, passive acoustic sensors, and dispersed in a grid over the sea surface to search for undersea objects of interest. The first vehicle that picks up a signal and collects a sufficiently rich sample might pop-up in the air high enough to form a network with nearby vehicles in order to perform real-time triangulation or time-delay-on-arrival (TDOA) calculations on the target

and to relay the information to nearby manned or unmanned surface or airborne assets. Vehicles in the flock could take turns flying and sensing to overcome the flight-endurance limitation, and the use of mesh networking technology would make this exchange transparent to the world. During times of flight, they may relocate using a leap-frog approach to follow a moving target, or while floating the flock would measure the strength and direction of the current, and may then take advantage of the current for energy-efficient travel during repositioning.

With a metal detecting payload the same flock might be used to search shallow-water and beach areas for mines, potentially sacrificing themselves to detonate detected munitions. At sea they might be used to track ocean currents for oceanographic or meteorological studies [6], or to track boundaries of chemical spills [7]–[9], and would retain the ability to pop-up to acquire imagery or other data at elevations above the sea surface. Another operationally relevant application might be to aid in geo-positioning of underwater autonomous vehicles or assisting divers by creating a pseudo-GPS acoustic network [10]. Here members of the flock would acoustically transmit their own GPS fix along with a time stamp. The underwater users would collect this data from multiple members of the flock, and then perform a TDOA calculation to estimate their own position. There may also be non-passive missions; for example the flock might be used for deception [11], using an array of members with synchronized acoustic transmissions, mimicking predefined target signatures.

On the civilian side, fish and aquatic mammals [12], [13] are frequently fitted with GPS beacons so that marine biologists can track them when they surface, but they cannot be tracked this way underwater. Complementing the GPS beacon with an acoustic beacon would enable the flock of Aqua-Quads to track the animals underwater as well.

In the remainder of this paper details are provided on the development process to include design considerations and constraints, tools for estimating performance during the initial concept design phase, complimented by actual experimental data as the project evolved. It concludes with a look at the path ahead for outdoor testing, flights off water, sensor integration, and integration of cooperative behaviors. The initial work [4] and companion paper provide additional insight into the software and algorithm developments to support mission-level goals, cooperation between multiple agents, energy-optimal path-planning, sensor fusion for target identification and tracking [5].

II. CONCEPT DESIGN AND MODELING

As previously mentioned, the proposed platform is a fusion between a buoy for underwater sensing and an autonomous multi-rotor aerial vehicle; hardened sufficiently to survive in the marine environment for extended periods, and equipped with solar panels to recharge batteries during the daytime. The development of any robotic platform is an exercise in compromise, and for hybrid vehicles, compromise can often drive the design to a point where it is no longer of practical value. In early concept development discussions it was common for new desired features to enter the mix, but following sometimes heated debate on the potential risks and benefits, most of these ideas had to be rejected. The leading argument

for rejection was the requirement to survive in the marine environment, followed closely by the requirement to fly for a reasonable period each day. The ocean is devastating to machinery, therefore minimizing the number of moving parts exposed to the water was deemed critical, as the fouling of machinery would most likely be the limiting factor on vehicle lifespan. The requirement to fly is driven by the need for mobility separate from drifting. As will be discussed later in this section, flight-time per day will be limited by available energy as well as the efficiency of the platform as an aircraft. Efficiency is directly coupled to weight for anything that flies; therefore, weight had to be managed well, and this ultimately excluded many “nice-to-have” features. A discussion of the objectives and how they were met, as well as some initial, simplistic modeling are included in the remainder of this section.

A. Objectives and Design Considerations

The primary objectives were to develop a platform that could perform sensing at depths below the thermocline, that was able to fly for a reasonable period each day, and that could remain operational, unattended, for extended periods, on the order of weeks or possibly months. It is not difficult to see that these are all coupled in the design space. The need to survive in the marine environment for a length of time pushes the design toward minimal moving parts exposed to the water. The need to sense at depth requires the use of a tethered sensor that can hang far below the floating platform. The requirement to operate for extended periods requires extreme energy efficiency; however, flight is typically not efficient, so it is not reasonable to assume that expendable fuel or single-use-batteries could meet this requirement. The alternative is to absorb energy from the environment. The Wave Glider does this through extracting mechanical energy from wave motion, but this is not a technology that easily adapts itself for flight. Therefore, solar energy (also utilized on the Wave Glider) becomes the most practical source, but it is typically not a lot of energy, so this will constrain flight-time. Fixed-wing aircraft are generally far more efficient than VTOL aircraft due to the L/D advantage of a wing, where L is lift, and D is drag. Unfortunately, the requirement to operate autonomously at sea makes fixed-wing aircraft impractical in all but the calmest seas. Further, the tethered sensor would need to be retracted to enable a fixed-wing aircraft to take off and land, but on a VTOL aircraft the tethered sensor could remain deployed for the life of the platform, being a slung-load under the aircraft in flight. Flight speeds are expected to be low enough that this would not be an unbearable burden.

The ability of multi-rotors to take-off and land in swell and operate with a deployed sensor won out over fixed-wing vehicles, but the compromises included limited flight time and lower cruise speed. Multi-rotors are typically quite reliable, being about as close to a *solid-state* helicopter as possible. The only mechanical wear parts are the motor bearing, and they are typically rated for more time between servicing than the total expected flight-time of the platforms - assuming that exposure to seawater can be controlled (more on this later). The only moving parts are the propellers. Typically multi-rotors have an even number of rotors, usually 4, 6 or 8 - occasionally more. While the mean time between failure for brushless motors and the electronic speed controls (ESCs) is typically quite large, a

quad-rotor can not remain in controlled flight if a motor is lost, but a hex or octo-copter can as long as the copter is not near maximum weight. The ability to land gracefully if a motor is lost turns out not to be a big selling point for an unattended platform, since it will never be able to return to flight without being serviced.

The present authors had previous experience with a solar powered aircraft, TaLEUAS, where a small array of SunPower C60 cells [14] were used to power avionics and payloads for an autonomous glider that sought out and rode thermals in order to minimize the propulsion energy requirement. Due to knowledge and affordable sourcing of the SunPower cells, they were adopted for the prototype Aqua-Quad. The cells were approximately 125 mm square. Cut from a 160 mm diameter wafer; they had small corner areas missing from the square, reducing coverage efficiency losses. The large square form factor of the cells suggested the use of a quad-rotor over a higher propeller count, purely based on efficient distribution of array area in a minimal diameter, leaving clear space for the rotor disks. By stretching the rotors away from each other by 140 mm or so, an X-arrangement of cells was possible. For future extensions of this project, smaller cells might be considered, as they would allow for more efficient area coverage, and more flexibility in rotor count.

Energy storage is always a critical consideration for electric aircraft. Cell specific energy is normally the primary driver, in particular for solar powered aircraft that are intended to fly through the night. Unfortunately, VTOL aircraft are power hungry, and the requirement for power-density generally precludes the use of battery technologies with the highest specific energy, as they typically have low power densities. Some of the COTS 18650 Li-Ion cells have specific energies up around 250 Wh/kg [15], but they generally only achieve this at a low discharge rate. They are usually designed for products like laptops and electric cars, where a normal drain-rate is something like a 5 h discharge time (referred to as 0.2C). As the drain-rate increases, the real specific energy of these cells falls due to voltage drop resulting from their relatively high internal resistance. If they are drained too quickly, this becomes a serious liability, as the internal resistance will lead to internal heat generation, and in extreme cases the cell can experience thermal runaway and ignition. Multi-copters rarely exceed about a 30 min flight time, as the battery mass-fraction becomes overwhelming; therefore, a cell that operates well at 3C or higher loads had to be considered. This ruled out currently available 18650 cells, and led the team back to prismatic Lithium-Polymer (LiPo) cells. This type of cell is prolific in the model aircraft market, with drain-rates as high as 80C available. LiPo cells also suffer from the inverse relationship between specific energy and power density, but readily available cells produce specific energies of about 195 Wh/kg at drain rates of 3C or more, and are capable of drain rates up to 15C or more without incurring damage.

B. Modeling

Long term goals will likely change, but for the prototype the team wanted to keep the platform as small as was practical. There are a number of non-scaling entities; for example, the autopilot, communication equipment, payload components, etc. The prototype needed to be large enough so that the

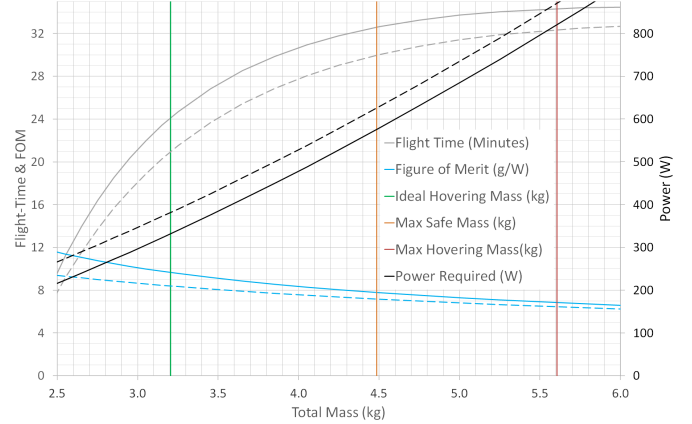


Fig. 2: Simple model predictions of performance.

mass fraction of these elements was not too significant. A simple modeling tool was constructed in spread-sheet form that included momentum theory [16] along with a number of empirical coefficients to allow for total weight and flight-time estimates based on parameters like rotor count and diameter, avionics and payload weight and power consumption. Empirical coefficients included simple scaling parameters like the structural weight as a function of motor weight, motor thrust as a function of motor weight, etc.

Momentum theory is the least conservative estimate of VTOL performance. It only considers the momentum lost in the wake; therefore, considering every other component to be perfect. For hovering flight it yields Eq. 1:

$$P = \sqrt{\frac{T^3}{2\rho A}} \quad (1)$$

where P is the power, T is the thrust (weight), ρ is the air density, and A is the area swept out by the propellers (disk area). In practice, nothing can get close to this limit. Historical measurements of small, hobby-class multi-rotor vehicles have shown them to operate at around 30 to 40 percent of momentum theory, with larger copters getting up around 40 to 50 percent. As a point of reference (shown in a later section), real helicopters tend to operate at around 50 percent. Efficiency is defined here as the percentage of momentum theory that is achieved, and in the spread-sheet modelling tool, it is a user-defined parameter. Typical results are shown in Fig. 2.

The three vertical lines indicate the *Ideal Hovering Mass*, *Max Safe Mass* and *Max Hovering Mass*. For most multi-copters the ideal hovering mass falls in the range from about 20 percent for small racing copters up to perhaps 70 percent for large, heavy copters primarily intended for hovering flight. Here a value of about 57 percent was assumed. The max hovering mass is the point at which the motors are saturated, and the copter is no longer flyable, and the max safe mass is assumed to be 80 percent of the maximum thrust, allowing for some motor overhead for maneuvering. Vehicle mass increases along the horizontal-axis, and the estimated endurance, Figure of Merit (FOM) and power required, are plotted as the battery mass is increased. The solid lines represent data including solar input, and the dashed lines without. The FOM is defined here as the grams lifted per Watt of power. Empty weight of the

model is the point (off the left side of the plot) where the grey lines intersect the x -axis, roughly 2.25 kg. With enough battery to meet the *Ideal Hovering Mass* the vehicle should be able to fly for about 24 minutes on a charge with solar, or 21 minutes without, and if the battery mass is increased to the safe limit, roughly 32 minutes with solar or 30 minutes without.

With the increased payload and structural mass for the Aqua-Quad, compared to typical multi-rotors, the calculator predicts that the model will reach maximum mass before reaching a peak in maximum endurance. With lighter copters, this is usually not the case, and the calculator will show a diminishing endurance due to loss of efficiency at the higher disk loadings. The FOM at the ideal hovering mass is roughly 9.7 g/W with solar, or 8.4 g/W without, which are reasonable numbers for the proposed size of the copter. Higher numbers will improve endurance, but they generally only come about from lighter disk loadings. If the disk loading gets too light, the vehicle will become less agile, and will have more difficulty operating in turbulent air. Values between about 7 and 10 are typically acceptable.

The fidelity of the model at this stage is not great, but as components are selected, the empirical coefficients can be adjusted to improve the model accuracy. For this data a rotor diameter of 356 mm (14 in) was assumed, along with a base power requirement of 10 W for avionics and payload, and a 50 W influx from solar. A quick sketch in CAD suggested a quadrotor layout allowing for twenty SunPower cells, as shown in Fig. 3. SunPower E60 cells with an efficiency of approximately 24 percent were available suggesting a peak power intake of about 70 W, thus the 50 W estimate seems reasonable for less-than-perfect conditions. For reference, the SunPower C60 and E60 cells are typically not the cells used on rooftops. They have about a 20 to 25 percent higher efficiency, roughly at the top of the game for single crystalline Si cells [17]. There are certainly other cell technologies that can beat the E60s, but the cost of those cells is generally much higher. Of course higher efficiency cells would recharge the batteries more quickly, and provide a larger energy budget to allow for more flight time. For certain missions, the increase in flight performance may warrant the use of the more expensive cells.

The total flight time in a 24 hour period can be estimated by using historical solar irradiance data available on the National Renewable Energy Laboratory (NREL) website [18]. Flight operations for our team are usually conducted at Camp Roberts in central California. NREL provides archival data in the nearby city of Paso Robles, as shown in Fig. 4, with data for a full year shown in the upper plot, for the month of June in the center plot, and with all the days of June collapsed to a single, statistically-averaged day in the lower plot. Irradiance is shown on the vertical axes in W/m^2 , and integrating over time for the 24 hour period provides an estimate of the energy density (shaded area in the lower plot), with an estimated value of roughly 8200 Wh/m^2 . Multiplying this by the array area and the cell efficiency yields an estimate of the total energy available on an average day in June in Paso Robles, roughly 590 Wh. This energy will be consumed by avionics and payloads as well as flight. Assuming an average avionics/payload power requirement over the 24 hour period of 5 W, this consumes 120 Wh, leaving 470 Wh for flight. Using the power estimate from Fig. 2 of about 350 W at the

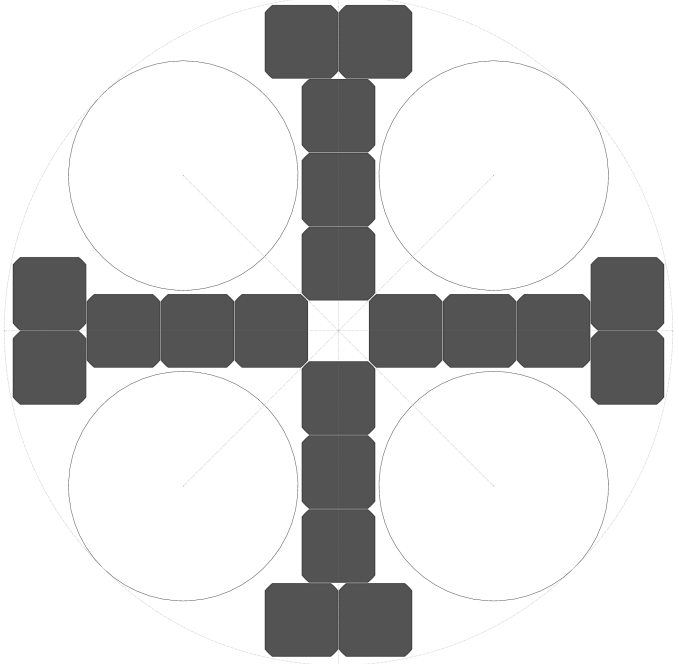


Fig. 3: Quad-rotor layout with 20-cell SunPower PV array.

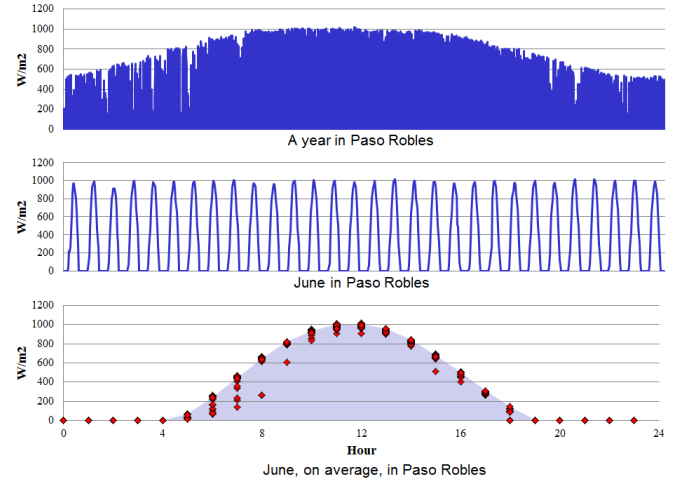


Fig. 4: Archival solar irradiance data for Paso Robles [18].

Ideal Hovering Mass, this suggests a total flight time in a 24 hour period of about 80 minutes. If flight speeds are on the order of 20 knots, then flight range per day is about 27 nm, resulting in a flight speed averaged over the 24 hour period of just over a knot, a value comparable to the Wave Glider in light sea states [19]. This estimate provides strong evidence of the need for intelligent hybrid mobility algorithms that optimize drift and flight segments.

Battery sizing can be driven by several factors. For example, it might be set to achieve the ideal hover mass, a maximum useful flyable mass, or to maximize solar absorption in a 24 hour period. In the end, it was set to the minimum size thought necessary to keep the avionics and payload components powered through the night. Assuming roughly 10 W for a 12 h period, and leaving about 20 percent of the rated capacity in reserve for battery health, suggests a

minimum battery capacity of about 150 Wh. The LiPo cells of interest are quantized, only available in a 2 Ah capacity (7.4 Wh). Two packs were desired for redundancy, and the packs would be either 3S or 4S, resulting in a best possible fit of 178 Wh (either 3S 8 Ah or 4S 6 Ah). While the raw cells have a specific energy of about 195 Wh/kg, assembled together with protective/balance circuitry installed, the effective specific energy falls to about 175 Wh/kg. This suggested a battery mass of roughly 1 kg.

The choice to base battery size on minimal night time requirements added some constraints to the operations. Night-time flight would be severely limited. The aircraft would need to land with enough reserves to keep the systems alive for the rest of the night, or potentially allow for system shutdown until the Sun came up the next morning. Also, the length of each flight leg would be limited. While the copter could fly for about 80 minutes in a day, a single flight leg would be limited by the available 178 Wh. For the estimated 350 W power required for flight, each leg would be no more than about 24 minutes, and with the estimated flight speed, this resulted in a range of about 8 nm per hop. A recycle time of about 3.5 hours between the hops would be required to top off the batteries. Both of these calculations assumed a 50 W solar power input as well as a 10 W avionics and payload power load.

All of these calculations were based on general principles, and for the most part were not specific to actual components. In the next section, a summary of the more specific component selection and prototype design will be given with individual experimental component performance results where possible.

III. PROTOTYPE DESIGN

In the previous sections, basic size and weight figures were derived through simple modeling techniques and some mission priorities. In this section those characteristics are refined into flyable and floatable prototypes. This is split into subsections for the propulsion system, energy management system, some basic details about the full Computer Aided Design (CAD) modeling, and the path from CAD to assembly using rapid fabrication techniques.

A. Propulsion System

The design modeling summarized above lead the team to a quad-rotor layout with 356 to 381 mm (14 or 15 in) propellers; both sizes fit suitably in the layout shown in Fig. 3. Several suitable motors were evaluated using a motor test stand, which captured voltage, current, thrust, RPM, and motor and ESC temperatures. Motors considered were the T-Motor 3510-13 700 kv [20], and a newer T-Motor model, the U3 [21], with essentially the same core, but an improved case and bearings, as well as the KDE 3510XF 475 kv and 715 kv motors [22], [23]. Advertised performance varied significantly, but the motors also had significantly different weights. The higher *kv* models would need to run on a 3S battery and preferably the smaller propeller, but the 475 kv motor, with the highest advertised FOM, would need to run on a 4S battery, and could easily handle the larger propeller.

In order to evaluate the motors on a level playing field, measured thrust from the motor test stand was adjusted to remove the weight of the motor, propeller and ESC for the

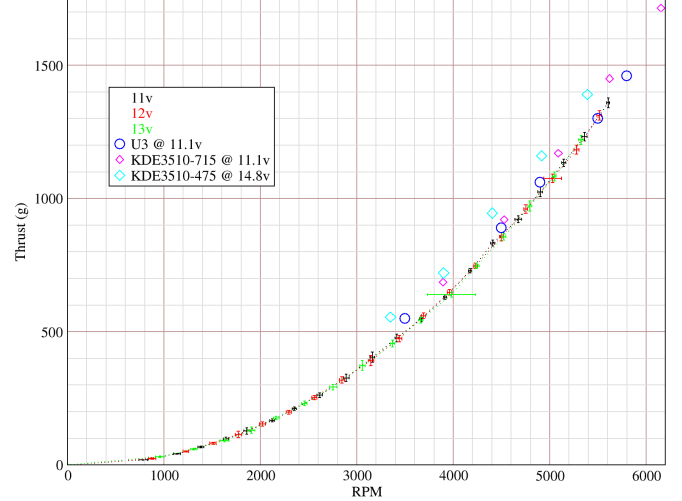


Fig. 5: Thrust as a function of RPM for the 15x5 propeller.

purposes of computing the FOM. The logic was that thrust required to lift the weight of the motor-system was *overhead*, and only the thrust above that was of practical value. Motor tests for the two T-motor models were identical, so only the U3 performance is included here. In Fig. 5 a measure of the propeller performance is shown with thrust versus RPM, with comparisons to advertised performance from the motor companies (symbols). The data is for the T-Motor 15x5 propeller, and as expected, the data for the motors running at different voltages collapse to a single line. Of interest are the somewhat elevated performance values provided by the companies. The data provided by T-Motor was actually a quite good fit; less so for the KDE data.

In Fig. 6 a comparison of the raw and adjusted FOM as a function of thrust is shown for the three motors, and with both the small and large propeller on the 475 kv motor. The dotted lines are for the raw FOM measurements and the dot-dashed lines are for the adjusted FOM calculations. The error bars unfortunately get quite large for these calculations, as the FOM is a derived term comprising inputs from several measured quantities, each with a measured uncertainty. While the KDE motors look better than the U3 in the unadjusted FOM curves, when their added weight is considered, the difference is subtle or non-existent. However, the 475kv motor with the larger propeller (15x5) should perform better due to the larger disk area, and for thrust levels high enough for flight, it appears to be the winner. Also note that if the total vehicle mass is 3.2 kg, each motor will need to support about 800 g, and this is roughly at the peak value of the adjusted FOM.

Looking at the KDE3510-475/15x5 motor/propeller combination in a little more detail in Fig. 7, the measurements for several voltages are compared with the manufacturer's advertised data. Measurements for the different voltage levels are in good agreement, but well below the advertised performance. Discussions with the company suggested that variations in samples, for the both the motor and propeller, might be the cause of the discrepancy. Whatever the reason, this is clear evidence of the value of local experimental testing during the early design stages.

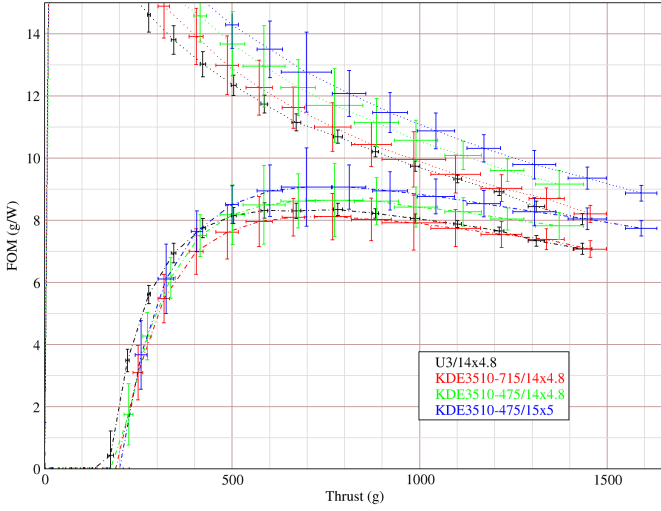


Fig. 6: Raw and adjusted figure of merit for several motor/propeller combinations.

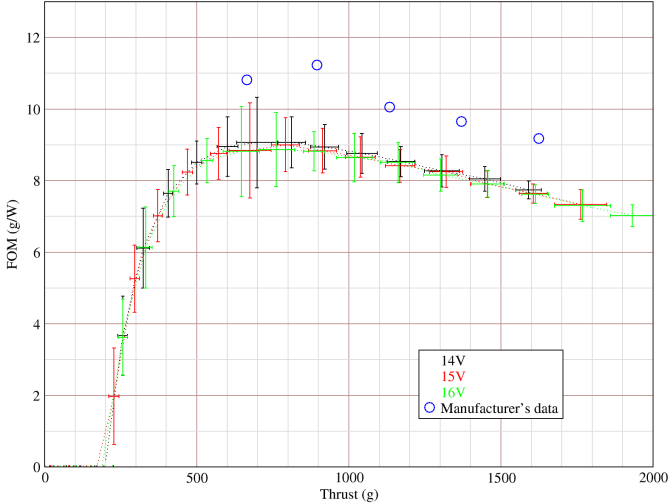


Fig. 7: Adjusted FOM for KDE3510-475 and larger prop.

B. Energy Management

The Aqua-Quad falls into a class of vehicles that the development team has coined *Energy-Independent*, meaning that their entire energy budget must be met by energy they harvest from their surroundings. In this case, the only source is solar energy through an array of monocrystalline Silicon photovoltaic (PV) cells. An energy flow chart with approximate component efficiencies is shown in Fig. 8. Here the MPPT is a Maximum Power Point Tracker with an embedded charge controller, and the BMS is a Battery Management System, a circuit that monitors pack and cell health, balances the cells, and attempts to prevent under/over-voltage and thermal runaway events. Some of the efficiencies are actual measured values, and others are based on data from the manufacturer or other sources, but the system estimates provide rough numbers to work from. In order to operate safely and effectively, the system needs to be aware of its energy state, in particular to make sure that sufficient energy is stored to keep the system alive through the night, and to estimate flight endurance at any

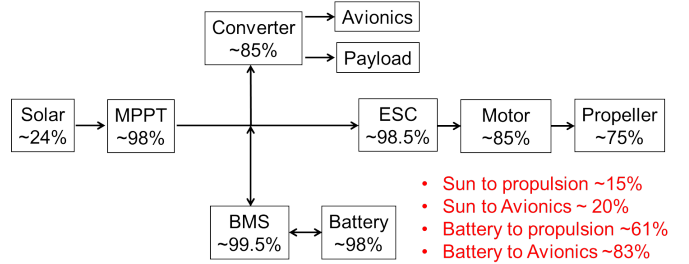


Fig. 8: Energy flow chart for the Aqua-Quad system.

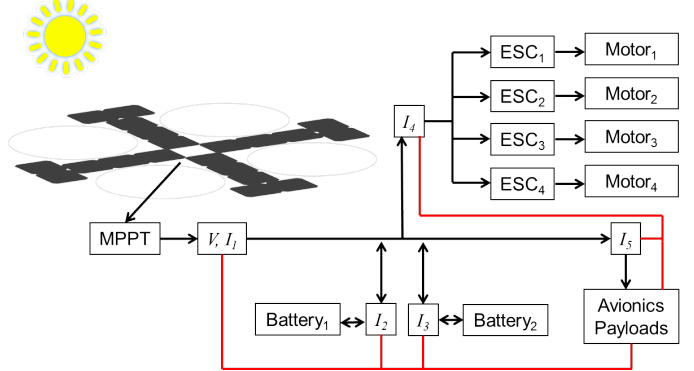


Fig. 9: System schematic with voltage and current sensors.

time. To provide the necessary data to the system, a printed circuit board (PCB) was fabricated that allows the payload computer to sample bus voltage and current flow at key points in the circuit, as shown in Fig. 9. The currents I_1 , I_4 and I_5 are all one-directional current measurements, but I_2 and I_3 are bi-directional, to sense the flow of energy in and out of the batteries. The BMS circuits have thermistors that monitor pack temperatures, but that information is not shared. Future versions of the PCB will likely add thermistor feedback to the payload computer as part of the health monitoring system. Similarly, when the PCB was designed, a single current sensor for all ESC/motors seemed appropriate, but recent advances in the quad-rotor racing community have resulted in very compact ESC options with built-in temperature and current sensors, and these may be adopted in the future.

Several MPPTs were evaluated for the project. Initially a GenaSun voltage boost model was tested [24]. It was an off-the-shelf model, but with a custom voltage output tuned for a 4S LiPo battery. It performed well, but, even stripped down to a minimal system, it was large ($12 \times 5.5 \times 2.5$ cm) and heavy (97 g). It included a large inductor and several large electrolytic capacitors as part of the output filtering circuit. In early testing of the MPPT, an unfortunate side effect of the large inductor was discovered. The proximity of the MPPT to the GPS/compass module caused a loss of compass data whenever the Sun was shining brightly. The compact aircraft chassis did not provide options to move the large MPPT further from the compass.

Another solution was discovered by a Naval Postgraduate School (NPS) student [25] in the way of a product evaluation board for an MPPT chip from STMicroelectronics, the SPV1020 [26]. The particular evaluation board shipped with three complete MPPT circuits wired in either parallel or series

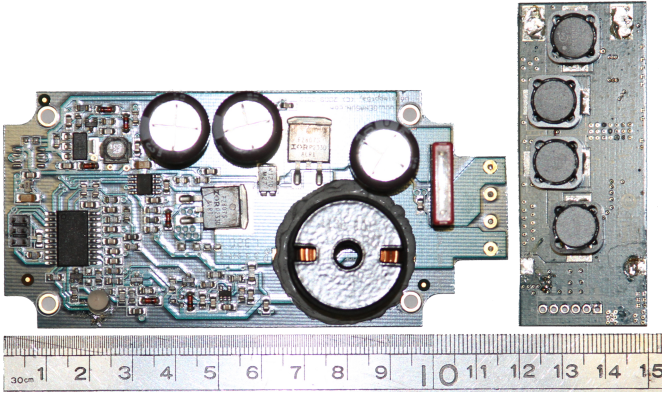


Fig. 10: GenaSun (left) and STM (right) MPPTs.

on a single PCB. It was discovered that the board could be cut into thirds to yield three separate MPPTs, making for a very compact and light solution ($7.5 \times 3 \times 1.1$ cm and 25 g). The two MPPTs are shown in Fig. 10 for reference. The STM board had four much smaller inductors and only used compact ceramic capacitors, and with some effort, the output voltage could be tuned to the required peak voltage of the 4S LiPo batteries by swapping four small (0603) surface mount resistors. The smaller inductors did not conflict with the compass, and the size of the board allowed it to be moved around in the chassis as needed. The evaluation board has been discontinued, but STM released the PCB layout, so potentially the circuit could be built into the PCB in future models. While the 73 g weight difference might seem insignificant to those unfamiliar with the design of flying machines, according to the spread-sheet model introduced earlier, the added 73 g results in a loss of about 90 seconds of endurance.

The complete charge circuit was tested on a slightly hazy, but mostly clear Monterey summer day. A pair of batteries were attached to the system with an initial at-rest voltage of about 14.7 (they were drained to 14.4 V with a 4 A load prior to being connected) and charged roughly to full. Shown in Fig. 11, the system voltage along with Watt hours stored are shown as functions of time. Power-in ran between about 50 to 60 W. As the battery reached the peak voltage of 16.8, the MPPT automatically tapered off power absorbed from the array, seen as the reduced slope in absorbed energy and the rapid drop in measured current and power. Scattered clouds during the first 20 minutes reduced the power intake, although the MPPT was quick to adapt to changing conditions. The batteries were essentially full after about 145 minutes. The autopilot and telemetry radio were running during the experiment, allowing for voltage as well as GPS and compass data to be monitored in the ground control station (GCS) during the experiment. This created a several Watt load throughout. In the 145 minutes, approximately 125 Wh were absorbed from the Sun. Using a pair of EagleTree eLogger V4s [27], one upstream and one downstream of the MPPT, estimates of the MPPT efficiency were in-line with manufacturer specifications, about 98 percent.

C. Full CAD Model

With the desktop fabrication techniques available today, the utility of CAD software for project design has taken on new

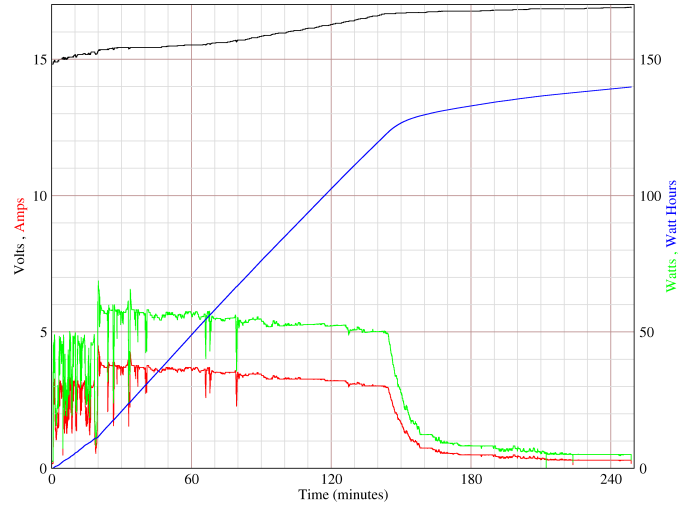


Fig. 11: Evaluation of the MPPT charge circuit.

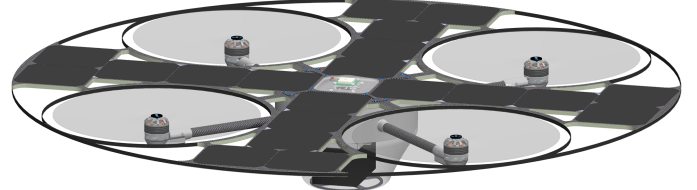


Fig. 12: Top view of the CAD model.

meaning. Certainly CAD has been useful for efficient component design, verification of system assembly, and estimates of weight, center of gravity and center of buoyancy; but with the ability to perform 3D printing and desktop machining of parts, the time to go from *idea* to *working model* has become a matter of hours instead of days, weeks or months. Knowledge of the materials and any inherent limitations or weaknesses in the fabrication methods is certainly needed, but the cost and time-line for prototype development has likely been reduced by an order or more. The full CAD design of the prototype is shown in Fig. 12 from the top, and in Fig. 13 from the bottom. The CAD model was fairly complete, just missing some minor wiring and electrical connections that are difficult to render in CAD. The total weight estimated in CAD was 2850 g, and the weight of the prototype was 2950 g - a 100 g error due to the un-modeled components. This was with the U3 motors and smaller propellers. The KDE motors and larger propellers will add an additional 125 g. This put the model a little under the ideal hovering mass, but did not include the payload. The payload is still under development, but is expected to be between 300 and 500 g. This leaves the model near the ideal hovering mass, and well below the max safe mass.

D. Model Fabrication

The prototype uses a mix of 3D printed, CNC machined, vacuum-formed, and stock or modified commercial off the shelf (COTS) parts. All printed parts are produced on a large-volume Fortus 400mc printer, and use their Polycarbonate (PC) print material. The PC parts are quite strong, remarkably isotropic for fused deposition modeling (FDM), and can be

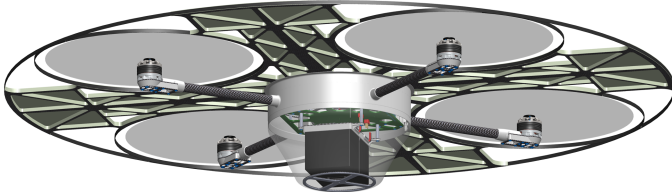


Fig. 13: Bottom view of the CAD model.

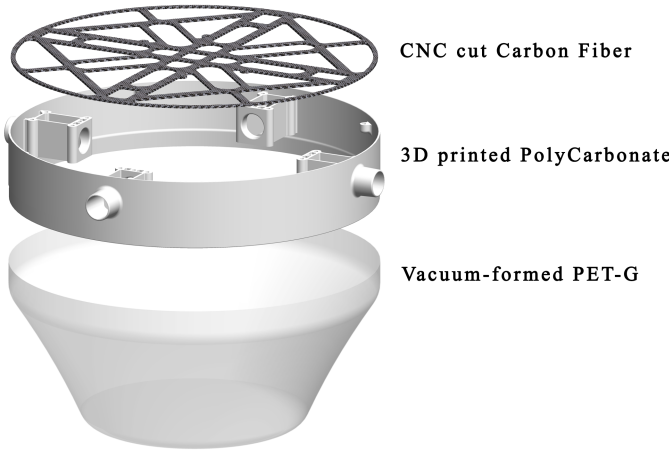


Fig. 14: Three CAD-to-fabrication techniques.

tapped and threaded reliably, even for small bolts. Printed parts do have several weaknesses. They typically need relatively thick walls for strength, they often are permeable to water, and the cost of the material is quite high. On the other hand, the complexity of the parts that can be made is nearly unbounded. However, for parts where much greater strength to weight is required, generally carbon fiber (CF) products are used, either prefabricated tubes or sheets. The sheets are typically CNC milled on a low-cost desktop machine. For essentially non-structural parts with complicated shapes that need to be impermeable to water, vacuum-formed PC or PET-G is useful. The molds for the vacuum-formed parts are generally 3D printed parts. Several parts from the frame core, typical of these fabrication techniques are shown in Fig. 14.

In the prototype the structural support for the solar array is fairly minimal; CNC cut from a CF-foam sandwich plate. The material is quite light, fairly stiff and safe in water. However, it will likely get replaced with a manufactured foam-core composite part in the future. The PV cells are marketed as rigid cells. In practice, they can handle some deflection, such as conforming them to the surface of a wing. If they are bent too frequently or too much, they may crack. Interestingly, due to the design of the cells, they often still function well even after being cracked, but if they develop an internal short, then the entire array is dead, and the Aqua-Quad will lose the ability to energize itself. The hope is that a molded composite part could have stiffness tailored as needed. It might also provide a cleaner airflow for hovering and high speed flight, and, lastly, it may allow for better control over the distribution of buoyancy. This aspect will be discussed in more detail in a later section.

E. Avionics and Payload

The remaining components to make the prototype flyable include the autopilot, ESCs, communication equipment, and payload computer. Presently the open-source Pixhawk autopilot is used, along with peripheral components: a 3DR GPS/compass module (Ublox Neo-7) which receives signals from both the GPS and GLONASS constellations, the 3DR telemetry radio (for prototyping only, for short-range communications to GCS) and a Spektrum-compatible satellite receiver (prototype only - for manual flight). The prototype uses Talon35 ESCs from Castle Creations (may switch to open-source BLHeliSuite ESCs in the future), an Odroid U3 single board computer (now discontinued - will be replaced in future versions), and a generic USB WiFi radio. In the future an Iridium modem will be added for global reach and low-bandwidth communications between multiple agents while they are floating. Antennas are challenging on the copter. Any antennas that stick above the solar array will cast shadows on part of the array, and since all cells are part of the same array, partial shadowing on one cell is equivalent to partial shadowing on all cells. Iridium satisfies the antenna requirement, using very small, *puck* antennas that have a similar form factor to conventional GPS antennas.

Antennas for WiFi are a challenge still to be met. When the copters are floating, the antennas will need to be above water, but when the copters are airborne, the antennas would work better below the aircraft where they have a clean line of sight to other agents floating on the sea surface. Several options have been considered, for example, a minimal dipole antenna might be mounted out on one of the propeller rings, as far from the arrays as possible to minimize the risks of array shadowing and antenna masking. If the required data throughput can be well controlled, it is possible that the aircraft could function on just Iridium, but this will require significant data reduction on the copter itself.

One last interesting option would be the use of Broadband Global Area Network (BGAN). Typically these radios require high gain antennas with a tracking solution, which would not be possible on a platform this size; however, researchers at the Georgia Tech Research Institute (GTRI) have recently developed very compact, flat, agile aperture antenna solutions that might make this possible on Aqua-Quad [28], although would require giving up some solar array space for antenna space. The developmental cost of this technology is not small, but once designed, the manufacturing costs are reasonable.

IV. PRELIMINARY EXPERIMENTAL TESTING

Initial experimental testing has been performed on several prototype models. A flyable prototype, complete except for the PV cells and the bottom of the water-tight enclosure, having legs instead, has been flown in the indoor high bay of the Center for Autonomous Vehicle Research (CAVR) at the NPS. Flight tests have allowed for the tuning of autopilot gains, and basic performance measurements of the complete vehicle. There is also a non-flying water-tight prototype that has allowed for outdoor, at-sea flotation evaluations. A third prototype is underway that will utilize the KDE motors, larger propellers and the PV array. The current prototype will have its water-tight compartment completed, and will begin flights off of the water.

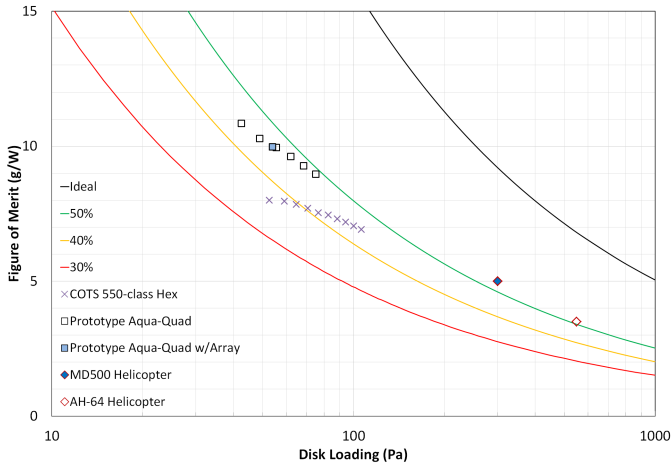


Fig. 15: Figure of merit versus disk loading.

A. Indoor Flight Tests

Measured performance of the flying prototype is shown in Fig. 15, with the Figure of Merit plotted against the disk loading, where the disk loading is the vehicle weight divided by the area swept out by the rotors. A log-plot is used for the disk-loading so that the performance of a few full size helicopters can be included for comparison. As before, the solid lines are based on momentum theory, with the black line representing the expected performance if the copter was 100 percent efficient. The green orange and red lines represent 50, 40 and 30 percent efficiencies, respectively. The two full size helicopters operate at just above 50 percent. The COTS 550 data points are performance from a 550 mm class hex-copter, where the variation in disk loading is obtained by adding lead weights to the model between short hover tests.

The Aqua-Quad prototype is much larger, and benefits from improved motor and propeller performance that comes from scale. The data point at the left is for a stripped model, missing the solar array support structure, the MPPT, all payload components, and using an undersized battery pack. As with the data for the 550-hex model, lead weight was progressively added to achieve higher disk loadings. The data point to the right is for a total weight of 3040 g, and required 340 W to hover. Also note that this data is for the U3 motor and the smaller propellers. This is a total weight that is slightly higher than the total weight for the complete prototype with this motor set. There is a single data point for the prototype with the solar array support structure attached. The interest here was to see if the addition of the structure adversely affected the hovering performance, and it does not appear to.

B. Open Water Flotation Tests

Routine flotation tests are performed in a small tank located in the CAVR to check for leaks and basic flotation. For a more real-world evaluation, a student-run experiment took the non-flying water-tight prototype out onto Monterey Bay to evaluate flotation in swell [29]. An Acousonde [30] sensor was attached to the bottom of the Aqua-Quad by a nylon cord tether. While the Acousonde is not the intended sensor going forward, it provided a suitable anchor-like influence on the flotation. The model included the PV array support structure,

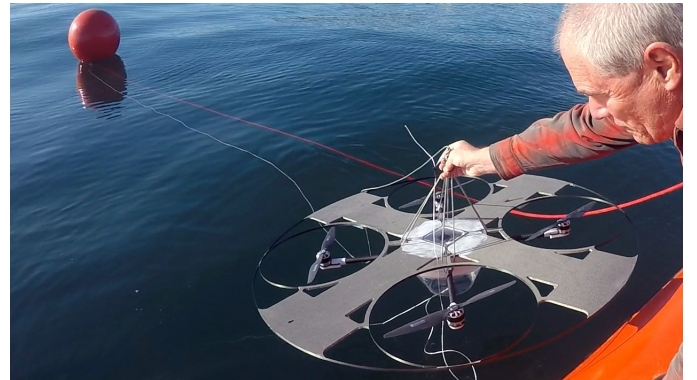


Fig. 16: Deploying the Aqua-Quad from a NPS RHIB.



Fig. 17: The Aqua-Quad in placid waters.

but not the PV cells, and was loaded with ballast to bring it up to the expected flying weight. The deployment from a NPS RHIB is shown in Fig. 16, and at rest in placid waters (≈ 1.25 m swell) in Fig. 17. In case things didn't turn out as expected, the Aqua-Quad was tied-off to a buoy with about 20 m of cord. Of particular interest was the stability. If the Aqua-Quad did not stay level with the water surface through swell, parts of the solar array would be underwater routinely in significant swell, and this would impede its ability to recharge. Careful distribution of buoyancy under the array provided the necessary stability. After a short run in calm seas, the Aqua-Quad was retrieved and then redeployed further out in the bay where it experienced swell over 4 m, but with light winds and no breaking waves, still behaving well.

V. CONCLUSIONS AND FUTURE WORK

This paper presented something of a progress report on the development of the novel, hybrid Aqua-Quad platform, with a brief summary of the goals, and the decision process that led to the current configuration. Simple modeling tools were developed to aid in estimation of power required for flight, endurance, and total flight-time in a day, and experimental testing of individual propulsion components helped guide the selection of materials for the prototypes. Several prototype models were produced, taking full advantage of modern rapid fabrication techniques for quick CAD-to-part turn-around. A flyable, non-water-tight model has demonstrated flight performance close to or slightly better than the model predictions. Electrical system tests have demonstrated solar recharging of the protected battery pair, providing solar performance in line

with manufacturer specifications and statistical irradiance data from the National Renewable Energy Laboratory.

Ongoing efforts includes further hardening of the system for marine environment, following the efforts of researchers on the Corrosion Resistant Aerial Covert Unmanned Nautical System (CRACUNS) project [31], and their use of COTS hydrophobic coatings. Additionally, since the Aqua-Quad will spend most of its time floating, it needs to be passively self-righting in case it is flipped in heavy sea states. Work is being done to optimize the distribution of mass and buoyancy, such that with the small correcting moment that the tethered sensor will create as the tether hangs over the propeller guard on an inverted copter, the vehicle will right itself with no energy requirement or outside intervention. Flight clearances are in the works to allow for outdoor autonomous flights off dry land and water. Lastly, efforts are underway to develop suitable underwater sensors and payload components.

VI. ACKNOWLEDGMENTS

The authors would like to acknowledge the support provided by the Consortium for Robotics and Unmanned Systems Education and Research (CRUSER). Also, we are grateful to Prof. Kevin Smith at the Physics Department of the NPS for insightful and operationally relevant technical discussions that significantly reshaped the original concept of the work.

REFERENCES

- [1] C. C. Eriksen, T. J. Osse, R. D. Light, T. Wen, T. W. Lehman, P. L. Sabin, J. W. Ballard, and A. M. Chiodi, "Seaglider: A long-range autonomous underwater vehicle for oceanographic research," *IEEE Journal of Oceanic Engineering*, vol. 26, no. 4, pp. 424–436, 2001.
- [2] V. Dobrokhodov, K. Jones, and N. Camacho, "Cooperative autonomy of multiple solar-powered thermal gliders," in *World Congress*, vol. 19, no. 1, 2014, pp. 1222–1227.
- [3] K. Jones and V. Dobrokhodov, "Hybrid mobile buoy for persistent surface and underwater exploration," U.S. Patent 9,321,529, April 26, 2016.
- [4] C. H. Dillard, "Energy-efficient underwater surveillance by means of hybrid aquacopters," Master's thesis, Monterey, California: Naval Postgraduate School, 2014.
- [5] V. Dobrokhodov, K. Jones, C. Dillard, and I. Kaminer, "Aqua-Quad - solar powered, long endurance, hybrid mobile vehicle for persistent surface and underwater reconnaissance, part II - onboard intelligence," in *OCEANS 2016. IEEE Conference*, vol. 1. IEEE, 2016.
- [6] D. Johnson, R. Stocker, R. Head, J. Imberger, and C. Pattiaratchi, "A compact, low-cost gps drifter for use in the oceanic nearshore zone, lakes, and estuaries," *Journal of atmospheric and oceanic technology*, vol. 20, no. 12, pp. 1880–1884, 2003.
- [7] J. Clark and R. Fierro, "Mobile robotic sensors for perimeter detection and tracking," *{ISA} Transactions*, vol. 46, no. 1, pp. 3 – 13, 2007. [Online]. Available: <http://www.sciencedirect.com/science/article/pii/S0019057806000097>
- [8] ——, "Cooperative hybrid control of robotic sensors for perimeter detection and tracking," in *American Control Conference, 2005. Proceedings of the 2005*, June 2005, pp. 3500–3505 vol. 5.
- [9] D. Moroni, G. Pieri, O. Salvetti, and M. Tampucci, "Proactive marine information system for environmental monitoring," in *OCEANS 2015 - Genova*, May 2015, pp. 1–5.
- [10] M. Erol-Kantarci, H. T. Mouftah, and S. Oktug, "Localization techniques for underwater acoustic sensor networks," *IEEE Communications Magazine*, vol. 48, no. 12, pp. 152–158, December 2010.
- [11] R. Lillbacka, "A swedish ebbinghaus illusion? submarine intrusions in swedish territorial waters and possible soviet deception," *Intelligence and National Security*, vol. 25, no. 5, pp. 656–681, 2010. [Online]. Available: <http://dx.doi.org/10.1080/02684527.2010.537122>
- [12] G. Schofield, C. M. Bishop, G. MacLean, P. Brown, M. Baker, K. A. Katselidis, P. Dimopoulos, J. D. Pantis, and G. C. Hays, "Novel GPS tracking of sea turtles as a tool for conservation management," *Journal of Experimental Marine Biology and Ecology*, vol. 347, no. 12, pp. 58 – 68, 2007. [Online]. Available: <http://www.sciencedirect.com/science/article/pii/S002209810700158X>
- [13] J. Ward, M. Fitzpatrick, N. DiMarzio, D. Moretti, and R. Morrissey, "New algorithms for open ocean marine mammal monitoring," in *OCEANS 2000 MTS/IEEE Conference and Exhibition*, vol. 3, 2000, pp. 1749–1752 vol.3.
- [14] SunPower Corp. (Accessed:2016-07-29) SunPower C60 solar cell. [Online]. Available: http://eshop.terms.eu/_data/s_3386/files/1379942540-sunpower_c60_bin_ghi.pdf
- [15] Power Cartel. (Accessed:2016-07-29) Test results for LG INR18650-MJ1 3,500mAh 18650 Li-ion battery. [Online]. Available: <http://powercartel.com/2015/02/test-results-for-lg-inr18650-mj1-3500mah-18650-li-ion-battery/>
- [16] Wikipedia. (Accessed:2016-07-29) Momentum theory. [Online]. Available: https://en.wikipedia.org/wiki/Momentum_theory
- [17] National Renewable Energy Laboratory. (Accessed: 2016-07-26) Best research cell efficiencies. [Online]. Available: http://www.nrel.gov/ncpv/images/efficiency_chart.jpg
- [18] ——. (Accessed: 2016-06-29) PVWatts Calculator. [Online]. Available: <http://pvwatts.nrel.gov/index.php>
- [19] R. N. Smith, J. Das, G. Hine, W. Anderson, and G. S. Sukhatme, "Predicting wave glider speed from environmental measurements," in *OCEANS'11 MTS/IEEE KONA*, Sept 2011, pp. 1–8.
- [20] T-Motor. (Accessed: 2016-07-26) T-Motor MN3510 specifications. [Online]. Available: http://www.rctigermotor.com/html/2013/Navigator_0910/37.html
- [21] ——. (Accessed: 2016-07-26) T-Motor U3 specifications. [Online]. Available: http://www.rctigermotor.com/html/2013/Power-Type_0928/90.html
- [22] KDE Direct. (Accessed:2016-07-26) KDE3510XF-475 brushless motor for electric multi-rotor (sUAS) series. [Online]. Available: <https://www.kdedirect.com/collections/xf-multi-rotor-brushless-motors/products/kde3510xf-475>
- [23] ——. (Accessed:2016-07-26) KDE3510XF-715 brushless motor for electric multi-rotor (sUAS) series. [Online]. Available: <https://www.kdedirect.com/collections/xf-multi-rotor-brushless-motors/products/kde3510xf-715>
- [24] G. LLC. (Accessed:2016-07-26) GV-Boost — 105-350w solar boost charge controller with MPPT. [Online]. Available: <http://genasun.com/all-products/solar-charge-controllers/for-lead/gvb-8a-pb-solar-boost-controller/>
- [25] R. T. Fauci III, "Power management system design for solar-powered UAS," Master's thesis, Monterey, California: Naval Postgraduate School, 2015.
- [26] STMicroelectronics. (Accessed:2016-07-26) Interleaved DC-DC boost converter with built-in MPPT algorithm. [Online]. Available: <http://www.st.com/content/ccc/resource/technical/document/datasheet/db/97/75/0e/d0/7a/42/46/CD00275733.pdf/files/CD00275733.pdf/jcr:content/translations/en.CD00275733.pdf>
- [27] Eagle Tree Systems, LLC. (Accessed:2016-07-29) eLogger V4. [Online]. Available: http://www.eagletreesystems.com/index.php?route=product/product&product_id=54
- [28] A. Robinson. (Accessed:2016-07-26) GTRI agile aperture antenna technology is tested on an autonomous ocean vehicle. [Online]. Available: <http://www.rh.gatech.edu/news/217981/gtri-agile-aperture-antenna-technology-tested-autonomous-ocean-vehicle>
- [29] L. R. Cason III, "Continuous acoustic sensing with an unmanned aerial vehicle system for anti-submarine warfare in a high-threat area," Master's thesis, Monterey, California: Naval Postgraduate School, 2015.
- [30] Acousonde, "Acousonde-3a underwater acoustic recorder," http://www.acousonde.com/downloads/Acousonde3A_Brochure.pdf, accessed:2016-06-29.
- [31] G. Brown. (Accessed:2016-07-29) New UAV can launch from underwater for aerial missions. [Online]. Available: <http://www.jhuapl.edu/newscenter/pressreleases/2016/160317.asp>